Non-Native Block Copolymer Thin Film Nanostructures Derived From Iterative Self-Assembly Processes

Nils Demazy, Cian Cummins, Karim Aissou, Guillaume Fleury

Non-Native Block Copolymer Thin Film Nanostructures Derived From Iterative Self-Assembly Processes

Nils Demazy[1], Cian Cummins[1], Karim Aissou[2], Guillaume Fleury[1,*]

[1]Univ. Bordeaux, CNRS, Bordeaux INP, LCPO, UMR 5629, F-33600, Pessac, France

[2]Institut Européen des Membranes, Université de Montpellier - CNRS - ENSCM, 300 Avenue du Professeur Emile Jeanbrau, F-34090 Montpellier, France

E-mail: gfleury@enscbp.fr

Abstract

Nanostructured block copolymer thin films constitute an elegant tool to generate complex periodic patterns with periodicities ranging from a few nanometers to hundreds of nanometers. Such well-organized nanostructures are foreseen to enable next-generation nanofabrication research with potent applications in the design of functional materials in biology, optics or microelectronics. This valuable platform is, however, limited by the geometric features attainable from diblock copolymer architectures considering the thermodynamic drive force leaning toward the formation of structures minimizing the interface between the blocks. Therefore, strategies to enrich the variety of structures obtained by block copolymer self-assembly processes are gaining momentum and this progress report reviews the opportunities inherent to iterative BCP self-assembly by considering the emerging strategies for the generation of "non-native" morphologies.

1. Introduction

Block copolymer (BCP) self-assembly is an elegant tool to generate complex periodic structures with exquisite symmetries. The driving force inherent to BCP phase behavior is related to the thermodynamic incompatibility between the two or more chemically distinct building blocks allowing BCP chains to microphase-separate into a panoply of well-ordered nanostructures with periodicities ranging from a few nanometers to hundreds of nanometers.[1–3] Innovative polymerization methods capable of generating on-demand BCP architectures associated to the conceptual framework of self-consistent field theory (SCFT) enable the rationalization of the rich bulk phase behavior of BCPs over the last decades, with, for the most simple di-BCP phase diagram, a progression of morphologies from spheres arranged into a body-centered cubic (BCC) lattice, hexagonally-packed cylinders, double gyroid, and lamellae.[1,4–6] As virtually any combination of chemistry and sequencing is attainable by macromolecular design,[3] BCPs offer tremendous opportunities for the design of functional materials with applications in biology, separation process and nanotechnologies among others.[7–9]

Further opportunities in the development of BCP nanotechnologies are linked to the formation of well-ordered periodic nanoscale patterns in thin film configuration with nanolithography as the "flagship" application. Indeed, the chemical dissimilarities between the domains allow selective removal by plasma or wet etching of one of the BCP domains leading to a mask that can be further used to define features in microelectronic applications. The formation of self-assembled patterns in thin film can also be combined with hybridization methods,[10] thus converting the BCP patterns into functional structured surfaces such as bit-patterned media,[11–13] field effect transistors,[14,15] optical metamaterials[16–18] or photonic structures.[19–21] This can be performed by using the nanostructured BCP scaffold as a template

for a subsequent deposition of functional materials (*via* sequential infiltration synthesis,[22,23] electro- deposition or replication,[17,24–26] lift-off process[27,28], aqueous metal reduction[29,30], inclusion of nanoparticles,[31,32] sol-gel process,[33] etc.). Alternatively, co-assembly strategies can be employed in which the BCP self-assembly process acts as a structure directing agent for nano-objects[34–37] or metal-oxide precursors.[16,38–40] Most of the aforementioned applications require the precise positioning or registration of the BCP nanostructure arranged within a highly-ordered nanoscale array. However, even if the equilibrium energy state of a BCP morphology would be reached for a uniform array of single-grain BCP features, a polygrain BCP structure is generally observed in thin film due to the prevalence of slow coarsening kinetics over the thermodynamic driving force. This weak thermodynamic driving force pushed scientists to develop directed self-assembly (DSA) methods providing means to control the domain alignment and orientation occurring through defect annihilation at grain boundaries. Methods to dictate self-assembly in this regard include solvent vapor annealing (SVA),[41] unidirectional solution casting,[42] gradated thermal annealing via laser writing,[43] the application of external mechanical,[44,45] electrical[46,47] or magnetic[48,49] fields, the use of surface energy modifiers[50,51] and guiding patterns.[52,53] For instance, further progresses were achieved in DSA lithography by the synergistic combination of the "bottom-up" BCP self-assembly with the "top-down" fabrication of guiding patterned templates relying on chemoepitaxy[54,55] and graphoepitaxy[56,57]. The interested reader is referred to comprehensive reviews detailing these DSA methodologies and their implementation.[58–62]

Nevertheless, the geometric features attainable from di-BCP architectures are limited considering the thermodynamic drive force leaning toward the formation of structures minimizing the interface between the blocks, even if deviations from the bulk equilibrium structure have been observed in thin films due to boundary or commensurability effects.[63–67] Therefore, strategies to enrich the variety of structures obtained by BCP self-assembly

processes are gaining momentum in the BCP community.[3,68–70] A first strategy builds on macromolecular engineering by incorporating additional chemical blocks in complex architectures (from linear to star, brush, H-shaped or supramolecular) in order to bring morphological variety and advanced functional properties.[71–76] Another strategy is to design novel three-dimensional nanostructures with unique structural motifs and symmetries by a layering process derived from the iterative self-assembly of BCP layers. This layer-by-layer stacking of BCP patterns comes in a variety of multi-faceted processes as shown in **Figure 1**: application of a protective layer, direct deposition of a BCP layer on top of an immobilized one, crosslinking of the underlying pattern and transfer of a nanostructured film on top of an underlying one. The breadth of methods to generate these complex structures is directly linked to the advances in the control of BCP self-assembly in thin films through DSA and hybridization methods.

Here, we review the opportunities inherent to the iterative BCP self-assembly by considering the emerging strategies for the generation of "non-native" morphologies (i.e. BCP nanostructures deviating from the bulk equilibrium phase behavior). We will particularly focus on the methods allowing fine control of three-dimensional structures resulting from iterative self-assembly approaches. The emergence of three-dimensional nanoelectronic devices[77,78] highlights the importance of advancing nanofabrication methods to precisely position material stack layers. In this regard, there is a clear motivation to assess the potential of BCP materials that can be patterned to form "non-native" morphologies.[69] This progress report therefore centres on the most recent techniques disclosed in the BCP field that show promise to benefit a range of device applications. Finally, we highlight that such non-trivial structures could find applications in critical technological fields where precise three-dimensional placement is imperative including nanoelectronics (for integrated logic and memory features),[79,80]

membranes (for high active surface areas),[81] batteries (for ion transport)[82] and nanophotonics (for metamaterials).[21]

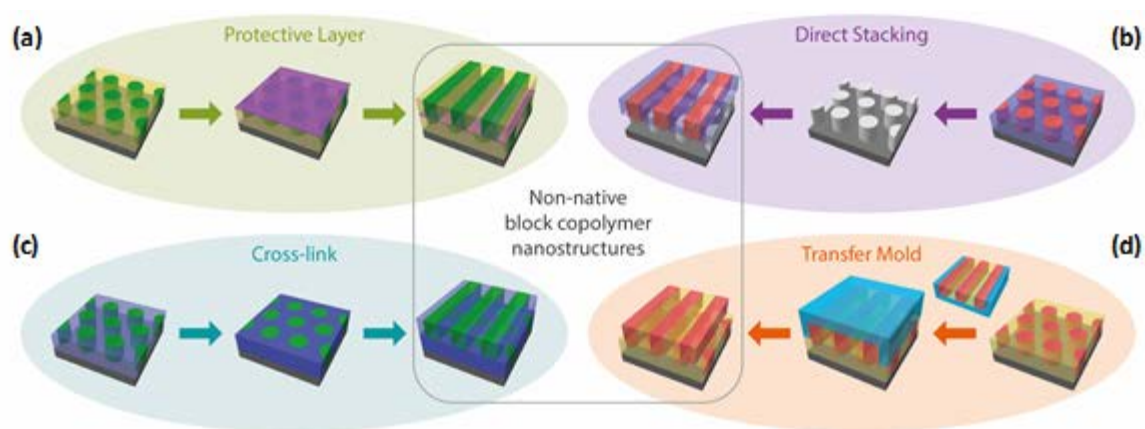**Figure 1.** Schematic illustration of various iterative self-assembly methods for the generation of three-dimensional structures beyond the native BCP morphologies. a) deposition of a nanostructured BCP thin film onto a protective layer, b) direct stacking of layered BCP structures *via* an immobilization method, c) stacking of cross-linked BCP patterns and d) BCP film transfer method on top of a nanostructured BCP layer.

2. Layering of block copolymer patterns

Pioneering works by Osuji and co-workers demonstrated how the deposition of BCP layers by electrospray suggests an ability for the formation of complex morphologies, only by selecting the sequence of BCP materials deposition.[83] Indeed, the deposition of sub-micron droplets formed by electrospray fluid atomization allows the continuous growth of BCP thin films providing a versatile approach to build composite layered BCP nanostructures. An exquisite demonstration was provided a few years later by Choo *et al.* with the production of lamellar heterolattices (i.e. lamellar stacks of varying periodicity) by sequential electrospray deposition of dilute solutions of poly(styrene)-*block*-poly(4-vinylpyridine) (PS-*b*-P4VP) chains having different molecular weights.[84] Interestingly, depending on the substrate temperature, distinct layers (sharp interface profiles) or gradated layers (smooth interface profile) were produced by altering the inter-diffusion of BCP chains, although orientation control and respective alignment of the BCP layers were not demonstrated.

A step forward for the formation of customized three-dimensional layered BCP structures was demonstrated *via* the definition of complex mesh patterns for which the control of the crossing angle allows the realization of all possible 2D Bravais lattice symmetries as shown in **Figure 2**.[85–88] Indeed, the orientation of different superposed layers of cylinders issued from BCP self-assembly can be directly controlled by topography to produce non-equilibrium morphologies in thin films. Tavakkoli *et al.* pioneered the fabrication of three-dimensional multilevel structures of cylinder arrays with controllable angles, bends and junctions whose geometries were dictated by periodic arrays of posts obtained by electron-beam lithography (see **Fig. 2a,b**).[85,89] In particular, they demonstrated how a periodic array of posts could independently control the orientation of individual layers of cylinders in BCP bilayers through the control of the chemical affinity between the posts and the BCP domains. An exceptional combinatorial

control over the final structure was achieved by fine tuning of post array geometrical features allowing the fabrication of various aperiodic mesh arrays. As a result, three-dimensional cross-point structures, highly attractive for the fabrication of memory arrays, were formed through the connection between cylinders of different layers.[85]

Several other processes have been described in the literature to obtain these multi-layered mesh patterns using either film transfer methods or iterative self-assembly of BCP layers. Nano-transfer printing of BCP layers, allowing a long range ordering of the BCP structure through the use of nano-patterned poly(dimethyl siloxane) (PDMS) mold have been demonstrated by Jeong *et al.* on various type of conformable substrates (indium tin oxide (ITO), Kapton®, poly(3,4-ethylenedioxythiophene):poly(styrene sulfonate) (PEDOT:PSS)).[86] This method allows the sequential printing of BCP layers on patterned substrates while selecting the crossing angle through the transfer process of the second layer (**Fig. 2c,d**). Another demonstration of film transfer process was proposed by Abate *et al.* who deposited a free-standing cylinder-forming BCP monolayer on top of a shear-aligned one.[90] The underlying cylinder layer acts then as a seed site to control the ordering of the final assembly during a subsequent thermal annealing step, highlighting the strong orientation coupling induced by the bottom layer.

BCP layers can also be independently stacked through the use of intercalated silicon or graphene separation layers (see **Fig. 2e,f**).[87,91] Likewise, both chemoepitaxy and graphoepitaxy which provide long range ordering of the BCP structure have proven to be compatible with such processes, to direct the orientation of mesh arrays. In particular, Kim *et al.* demonstrated how a chemically modified graphene layer can be used to screen the topographical and surface energy modulations induced by an underlying gold pattern obtained from nanostructured BCP thin film. The overlay of a second nanostructured BCP thin film on top of the separation layer generates a double layer gold mesh pattern without epitaxial registration between the layered structures. Interestingly, by combining such a method with

DSA, square array of dots, widely required for microelectronic device architecture, could be fabricated from mesh arrays *via* double steps of orthogonal etching.[87]
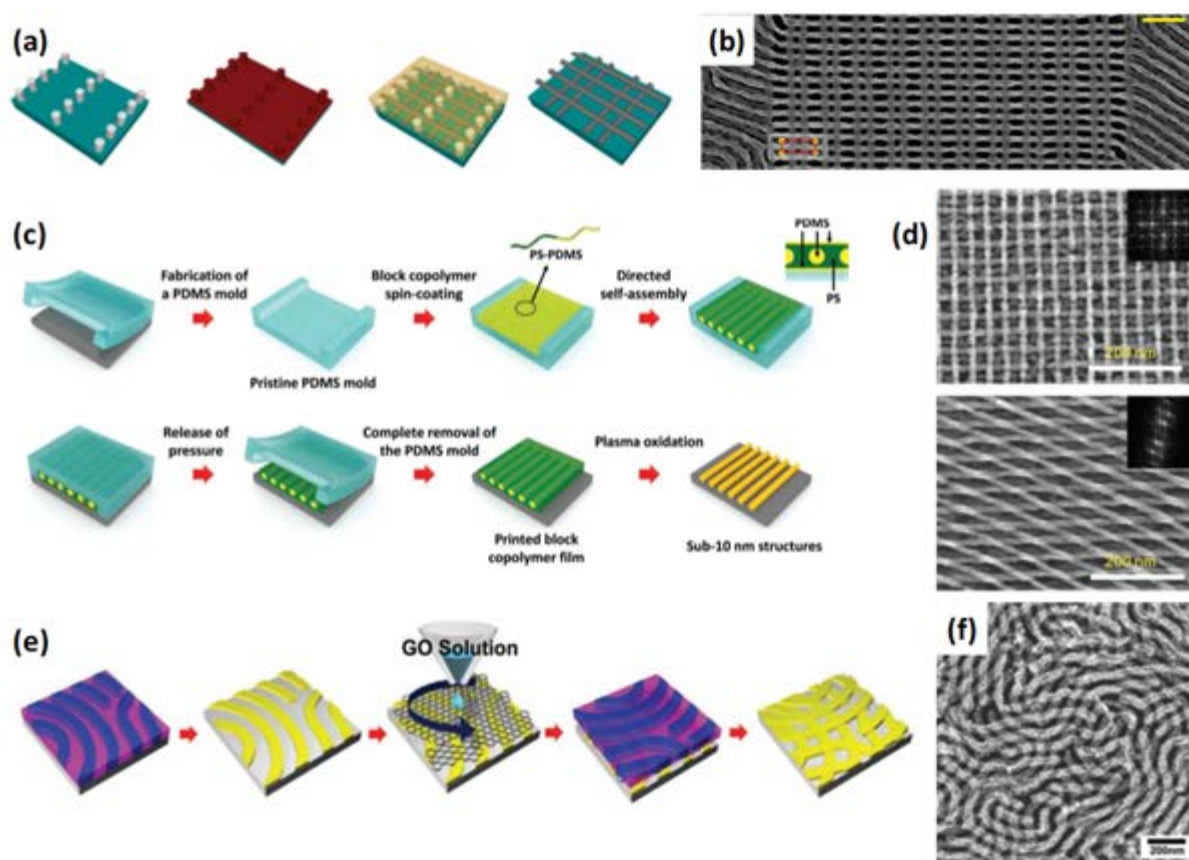

Figure 2. a,b) Schematic process flow for the fabrication of a bilayer BCP array using the post templating method and SEM image of the multilevel structure (scale bar: 100 nm): a cylindrical PS-*b*-PDMS bilayer is templated by an array of functionalized posts to form oxidized PDMS mesh structures after plasma treatment. Reproduced with permission.[89] Copyright 2014, Wiley-VCH. c,d) Process flow for nano-transfer printing of BCP patterns and SEM images of two double-layer mesh structures with different crossing angles: a patterned PDMS mold is used to guide the self-assembly of a PS-*b*-PDMS BCP followed by its transfer on a substrate. The sequential printing of BCP structures leads to mesh patterns with controllable crossing angle. Reproduced with permission.[86] Copyright 2012, Wiley-VCH. e,f) Gold mesh array fabrication procedure using a separation layer and SEM image of a double layer gold pattern: A protective chemically modified graphene layer is deposited on top of a gold nanowire pattern formed from BCP self-assembly which allows the deposition of a second nanostructured BCP layer. Reproduced with permission.[87] Copyright 2013, Wiley-VCH.

3. Crosslinking for sequential deposition of BCP patterns

Alternatively, BCPs can be designed to incorporate cross-linkable moieties into their architecture in order to immobilize the underlying BCP layers for a subsequent deposition process.[92–95] Pioneering works by Kim *et al.* using cylinder-forming poly(styrene)-*block*-poly(methyl methacrylate) (PS-*b*-PMMA) with reactive benzocyclobutene functionality inserted in the PS block have demonstrated how the stacking of cross-linked BCP patterns can be utilized to register the cylindrical domains of overlying layers formed on top of the underlying one (see **Fig. 3a,b**).[92] In an attempt to control the sidewall profile of nanostructures obtained from lamellar-forming PS-*b*-PMMA BCPs, He *et al.* reported vertically gradated structures for which the domain size was tuned by the addition of cross-linkable PS or PMMA homopolymers while keeping the registration between the stacked layers.[94] The non-native undercut (i.e. negative sidewall) profiles of the PS lamellar nanostructure resulting from the selective removal of the PMMA domains were proven to facilitate subsequent lift-off process for the formation of gold nanowires.

More sophisticated stacks obtained from cross-linkable BCPs were also reported by combining BCP layers with different morphologies. For instance, Jung *et al.* have demonstrated how lamellae-on-cylinders can be obtained from stacking a cross-linkable cylinder-forming PS-*b*-PMMA BCP layer with a lamellar-forming PS-*b*-PMMA BCP layer (**Fig. 3c,d**).[93,96] The study of the epitaxial relationships between both layers showed that the PMMA lamellae were remarkably registered to the underlying PMMA cylinders due to a favorable minimization of the interfacial free energies of the two BCP layers facilitated by the commensurability between their inter-domain spacings.

Figure 3. a,b) Schematics of the cross-linking and registration processes for stacked cylinder-forming PS-*b*-PMMA layers bearing reactive benzocyclobutene functionalities within the PS block and cross-sectional SEM image of a three layered BCP film in which the PMMA domains were etched by UV-exposure and acetic acid treatment. Reproduced with permission.[92] Copyright 2008, The Royal Society of Chemistry. c,d) Process flow for the formation of multilayered BCP nanostructures with controlled domain orientation produced from cross-

linkable BCP thin films and SEM image of a double-layer BCP structure consisting of an upper lamellar layer formed on an underlying cylindrical layer. Reproduced with permission.[93] Copyright 2011, American Chemical Society. e,f) Fabrication of nanoscale square patterns using cross-linked cylinder-forming BCP layers aligned by shear in a cross-pattern and SEM image a double-layered cross-bar pattern obtained after RIE treatment. Adapted with permission.[97] Copyright 2014, American Chemical Society. g,h) Schematic process flow for the fabrication of orientation-controlled three-dimensional multilayer structure and cross-sectional SEM image of a hierarchical templated structure consisting of a stack of out-of-plane lamellae, out-of-plane cylinders and a monolayer of in-plane cylinders: through filtered plasma treatment of an as-casted BCP thin film, a thin cross-linked layer is formed at the top surface while retaining the original chemical BCP composition. Such cross-linked layer can further act as a neutral top-coat for the underlying BCP layer or as neutral underlayer for a BCP layer deposited on top of it. Reproduced under the terms of the Creative Commons Attribution 4.0 International License.[98] Copyright 2019, the Authors. Published by Springer Nature.

Another simple method to create nanoscale cross-patterns (square, rectangular, and rhombic) over macroscopic areas was proposed by Kim *et al. via* shear-alignment of distinct layers of cylinder-forming polystyrene-*block*-poly(ferrocenylisopropylmethylsilane) (PS-*b*-PFiPMS) layers BCPs, immobilized through crosslinking using ultraviolet light (**Fig. 3e,f**).[97] The pattern symmetry could be adjusted through the variation of the cylinder-forming PS-*b*-PFiPMS pitches (i.e. rectangular *vs.* square) and through the independently set shear directions for the two layers (square *vs.* rhombic). This double-layered cross-bar pattern further serves as template for the definition of four-fold symmetry lattices of various features (nanowells, nanoposts, nanodots) using various etching and lift-off techniques.

Recently, Oh *et al.* have demonstrated how a cross-linked layer can also be applied to the fabrication of orientation-controlled 3D multilayer structures.[98] Through filtered plasma treatment of BCP thin films, a thin cross-linked layer was formed by the physical collisions of neutral species and retains the original chemical BCP composition, thus acting as a neutral top-coat for the underlying BCP layer or as neutral underlayer for a BCP layer deposited on top of it. The filtered plasma treated cross-linked layer is conceptually similar to a grafted brush layer

of random copolymers correcting the mismatch of surface energy between the BCP domains.[50] This approach combined with chemoepitaxy was applied to create hierarchical structures of chemically-different BCP patterns with the notable generation of arbitrary sequences of in-plane and out-of-plane features as shown in **Fig. 3g,h**. As a demonstration, Oh *et al.* fabricated a BCP stack similar to a fin field-effect transistor (FinFET) structure with sequential layering of out-of-plane lamellae and cylinders covered by a monolayer of in-plane cylinders connecting the apices of the vertical cylinders.

4. Immobilization of BCP pattern via hybridization methods for subsequent deposition of BCP structure

Advances in the formation of complex BCP structures from iterative self-assembly are related to the advent of various hybridization methods[10] leading to the immobilization of BCP structures. Indeed, the selective transformation of one of the BCP domains into oxides or metals combined with the removal of the BCP scaffold by wet or dry chemistries constitutes an original pathway for the production of non-native morphologies. For instance, Majewski et *al.* demonstrated fine control over the mesh pattern and symmetry through the conversion of polystyrene-*block*-poly(2-vinylpyridine) (PS-*b*-P2VP) patterns into metallic replicas, enabling the formation of non-native BCP thin film structures by successive layering of PS-*b*-P2VP thin films.[88] Photo-thermal annealing (i.e. laser-zone annealing) combined with soft-shear effects induced by an elastomeric pad was used to iteratively align the BCP structures, thus producing arbitrary lattice symmetries (**Fig. 4a,b**).

Further progress in the manipulation of iterative BCP self-assembly in thin films were demonstrated by exploiting a "responsive layering" approach[99] in which subsequent BCP

layers order as function of the underlying layers to generate complex three-dimensional structures. This method exquisitely exploits the natural propensity of BCP materials to respond to chemical or topographical fields. This intermediate "responsive layering" approach allows one to manipulate BCP self-assembly towards non-native three dimensional morphologies as each self-assembled BCP film acts as both a component of the final functional structure and a guiding pattern for the subsequent nanostructured layers. Consequently, immobilized BCP patterns can be used as a topographic or chemical template[100–102] for a subsequent BCP layer and complex three-dimensional structures can be obtained by iterative self-assembly of layers of BCPs with different molecular weights or compositions.[103–105] Tavakkoli *et al.* explored this particular facet for the formation of cross-point structures derived from self-assembly of BCPs with different periodicities.[104] A first PS-*b*-PDMS layer was self-assembled on a substrate leading to a topographic pattern of oxidized-PDMS cylinders after reactive ion etching (RIE) treatment. This grating pattern was subsequently used as a template to self-assemble a novel BCP layer which orthogonally aligned as regards to the previous layer due to weak chemical interactions between the oxidized-PDMS pattern and the BCP domains. Combining this orthogonal self-assembly process with circular or Y-junction lithographic patterns led to the fabrication of complex nanomesh structures as shown in **Fig. 4c,d**.

Another example of hierarchical nanostructures in which an immobilized BCP pattern acts as a guiding template for the self-assembly of a second BCP layer was provided by Son *et al.*[103] Using top-down methods to pattern a PS-*b*-PDMS BCP of large periodicity, they demonstrated how smaller period BCP patterns are registered on the larger BCP template. Following this methodology, line-on-line, dots-on-line and dots-in-hole hierarchical structures were produced depending on solvent annealing conditions as shown in **Fig. 4e,f,g**.
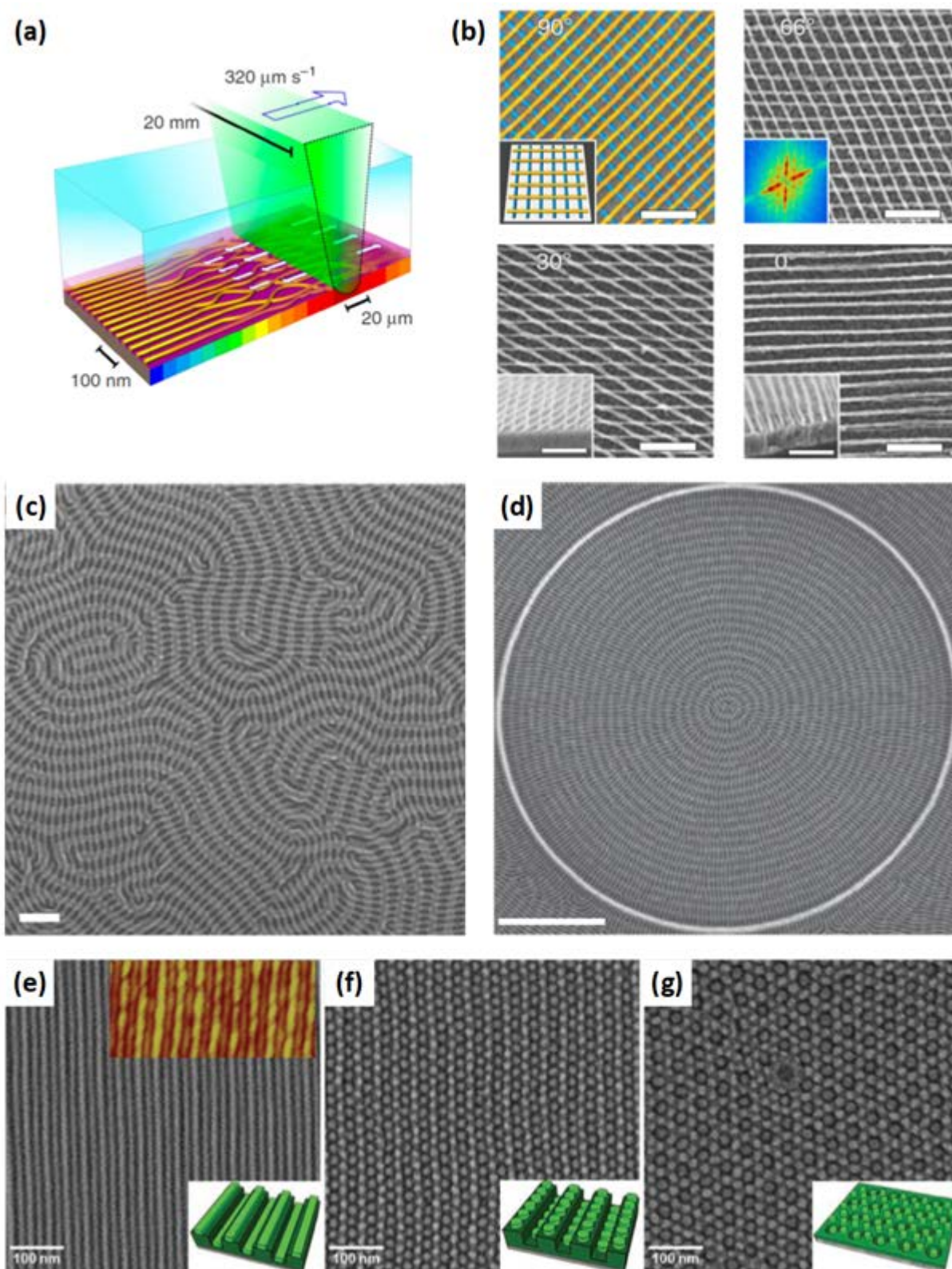
Figure 4. a,b) Schematics of photo-thermal annealing set-up combined with soft-shear effects (soft shear-laser zone annealing (SS-LZA)) for the alignment of BCP structures and SEM images of double-layered Pt mesh patterns obtained using various angles between the SS-LZA sweeps (scale bars: 200 nm). Reproduced under the terms of the Creative Commons Attribution 4.0 International License.[88] Copyright 2015, the Authors. Published by Springer Nature. c,d)

Nanomesh pattern obtained *via* orthogonal self-assembly of PS-*b*-PDMS BCPs of different molecular weights on bare Si (scale bars: 100 nm) and on a circular template obtained by electron beam lithography from a hydrogen silsesquioxane resist (scale bars: 500 nm), respectively. Adapted under the terms of the Creative Commons Attribution 4.0 International License[104] Copyright 2016, the Authors. Published by Springer Nature. e,f,g) Hierarchical structures including (e) line-on-line, (f) dots-on-line and (g) dot-in-hole made from a small period PS-*b*-PDMS BCP templated by a larger period PS-*b*-PDMS BCP. The different hierarchical structures were obtained by tuning the SVA conditions. Reproduced with permission.[103] Copyright 2011, Wiley-VCH.

Interestingly, the spherical BCP morphology has attracted particular attention for the realization of hierarchical structures from iterative self-assembly. For instance, density multiplication of single layer hexagonal silica dot pattern was demonstrated by Jin *et al.* through the stacking of plasma treated sphere-forming PS-*b*-PDMS monolayers.[106] A first monolayer of hexagonally close-packed dots was formed by spin-coating a highly asymmetric PS-*b*-PDMS BCP blended with PS homopolymer chains. The subsequent deposition of the BCP on top of this first plasma treated layer results in the formation of a dot pattern exhibiting a honeycomb lattice, since the dots of the second layer position themselves in the triangular interstitial positions of the first hexagonal pattern, as shown in **Fig. 5a,b**,. The dots formed by spin coating a third BCP monolayer on top of the oxidized honeycomb lattice registered to the hexagonal lattice positions resulting in a three-fold increase in dot density. The driving force governing the spatial positioning of the second and third layers of dots was linked to the topological constraints induced by the former dot layers. It is noteworthy that the addition of PS homopolymer chains was crucial to limit the dot overlap between layers, which is a primary concern for enabling density multiplication methodologies. Recently Jung *et al.* proposed a more direct approach to form dense dot layers from sphere-forming BCP thin films.[107] A double layer of PDMS spherical domains was formed by spin-coating a concentrated sphere-forming PS-*b*-PDMS solution in toluene. After plasma treatment, a distinct double pattern of hexagonally packed

silica dots was revealed through top-view SEM observation even if the two layers of dots were positioned at their respective sphere layer height (denoted as "pondering" pattern by the authors). Buriak's group pushed forward their studies on the sequential deposition of dot arrays formed by microphase-separated PS-*b*-PDMS thin films. Using BCPs having different periodicity, they studied the interrelationships between (in)commensurability and epitaxial alignment between different dot layers formed by following the same iterative deposition method of sphere-forming PS-*b*-PDMS layers. The sequential self-assembly of dot layers having different array pitches resulted in the formation of Moiré superstructures with preferential dot lattice orientation derived from the epitaxial registration of the top layer (see **Fig. 5c,d**).[108]
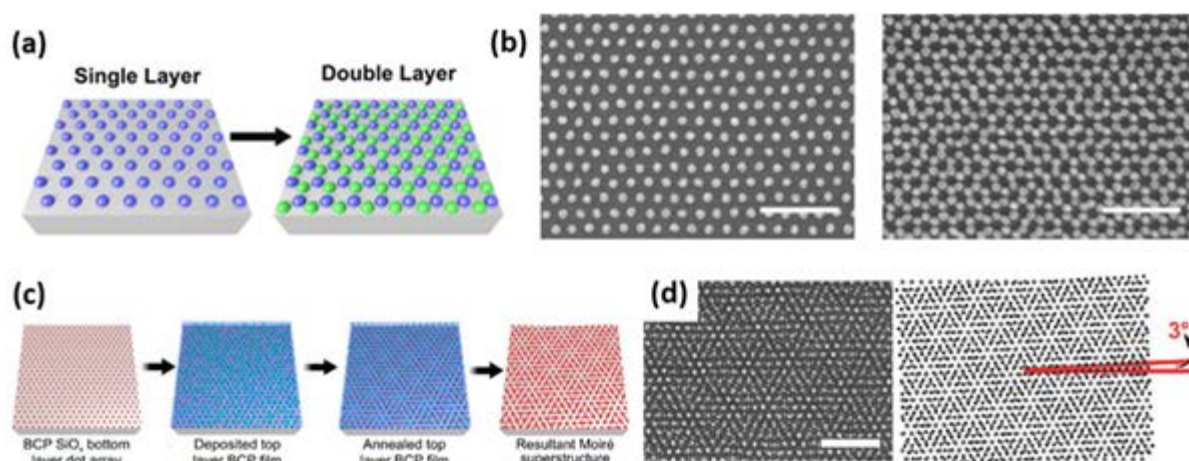

Figure 5. a,b) Sequential self-assembly process for the formation of density-doubled dot patterns from sphere-forming PS-*b*-PDMS BCP and SEM images of the single layer hexagonal and double layer honeycomb dot patterns (scale bars: 200 nm). Reproduced with permission.[106] Copyright 2016, American Chemical Society. c,d) Process flow for the fabrication of dot-array-based Moiré superstructures from sphere-forming PS-*b*-PDMS BCPs with different molecular weights and SEM image of a resulting structure with a relative rotation angle of 3° between the two layers (scale bar: 250 nm). Adapted with permission.[108] Copyright 2017, American Chemical Society.

Rahman *et al.* progressed further these methodologies by showing how "responsive layering" self-assembly allows access to a huge diversity of morphologies not native to the equilibrium BCP phase diagram, including square and rectangular mesh patterns, dots localized between nanopores, dots bridging lines. Their approach also relies on sequential deposition and immobilization of two-dimensional nanostructured BCP thin films but takes further advantage of a secondary registration field induced through the BCP chain stretching/compression (i.e. the second-layer morphology orients and registers so as to accommodate the underlying height variation by overlapping the interblock interface atop of it). As shown in **Fig. 6a**, the detailed process flow is based on the selective infiltration synthesis of nanostructured PS-*b*-PMMA thin films which generates a topographical pattern reproducing the BCP morphological features. After neutralization of the immobilized layer by a random copolymer brush to prevent chemoepitaxial replication, a second PS-*b*-PMMA layer is deposited on top of the underlying BCP pattern which self-assembles in response to the aforementioned topographical field. A striking demonstration was given by combinatorically stacking the three different classical two-dimensional BCP morphologies using PS-*b*-PMMA of different compositions and molecular weights resulting in a cornucopia of multilayered structures with a high level of spatial control (see **Fig. 6b,c**).
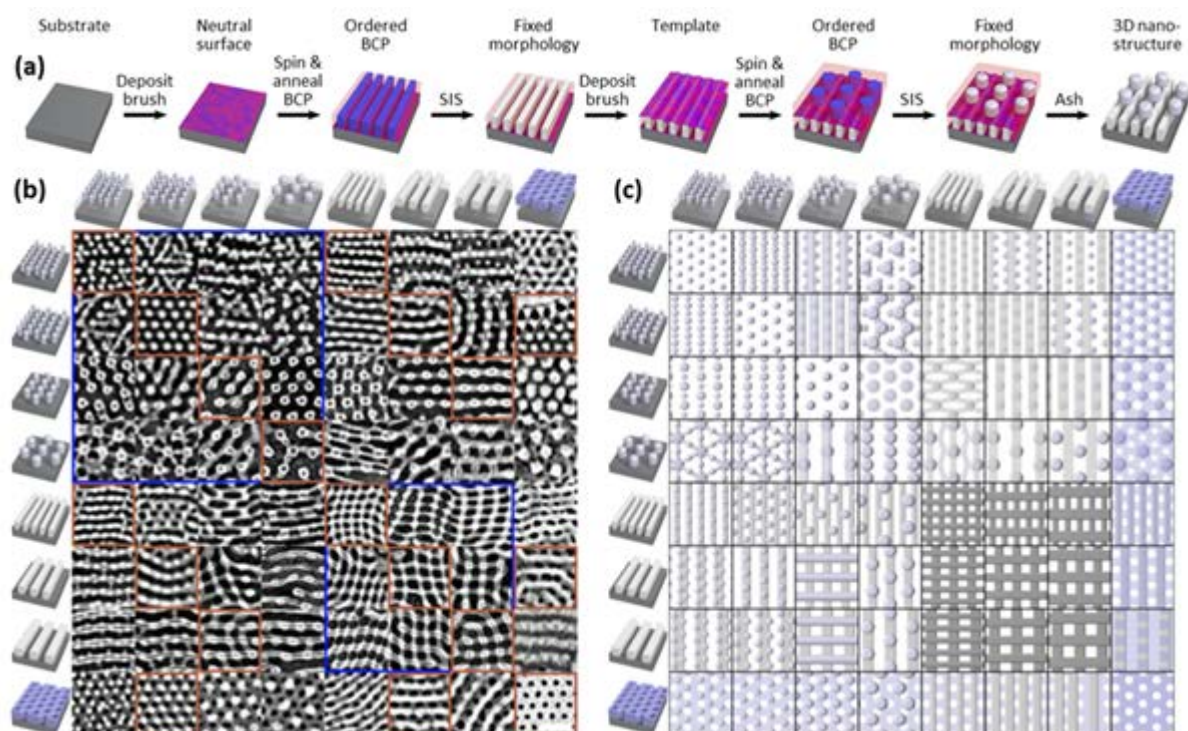
Figure 6. a) Process flow for the formation of three-dimensional nanostructures obtained from the "responsive layering" approach. b) SEM images showing the considerable diversity of two-layer nanostructures formed by the iterative self-assembly of BCP thin films using the "responsive layering" approach (scale bar: 100 nm). b) Schematics of the idealized three-dimensional nanostructures. Adapted under the terms of the Creative Commons Attribution 4.0 International License.[99] Copyright 2016, the Authors. Published by Springer Nature.

5. Conclusion and outlook

During the last decades, BCP self-assembly in thin film has enabled researchers in their quest to design ordered microstructures with nanometrically defined periodicity. Tremendous opportunities have emerged from these studies enabling the fabrication of functional materials from nanostructured BCP thin films; the most striking example being nanopatterning applications for semiconductor and memory uses. While directed self-assembly methods allow the generation of two-dimensional perfect ordered patterns, the intrinsic BCP phase behavior limits the variability of structures and symmetries achievable through BCP self-assembly. We have highlighted that iterative self-assembly in the form of stacking BCP layers allows access

to an enormous diversity of non-native morphologies beyond the classical bulk equilibrium di-BCP phase diagram. Such great progress in the design of multilayered hierarchical structures was enabled by both a deep understanding of the underlying mechanisms controlling the BCP self-assembly in thin film and the development of hybridization methods for the immobilization of the BCP patterns. It is noteworthy that theoretical and modeling efforts have provided guidance to expand the landscape of complex structures by assessing the critical parameters and design rules allowing the fine control of the multilayered BCP structures, and therefore is viewed as pivotal in future multilayer designs of non-native BCP morphologies. As a result, the BCP community faces up to a challenge in translating these novel complex structures into potent applicative advances with smart functionalities, as only a scarce number of the multilayered structures described herein has been transitioned to device manufacturing. For instance, three-dimensional nanostructures formed by directed self-assembly of BCP multilayers could be valuable in cutting-edge technologies such as optical metamaterials or metasurfaces,[21,109,110] graphene nano-ribbon or fin field effect transistors,[98,111,112] filtration membranes with improved permeability-selectivity trade-of[113–115], cross-point memories[85] or optoelectronic devices.[26,116] Additionally, the conversion of the BCP scaffolds into functional inorganic materials[10] broadens the scope of applications by adding specific optical, electronic or magnetic properties to the three-dimensional nanostructures.[21,70,117] Nevertheless, several challenges still need to be addressed for the advent of multilayered BCP structures in nanotechnology. Powerful DSA methods effective in the three-dimensional space are required for the precise registration of the BCP features, as such approaches will thus enable a high scalability of self-assembly processes. Understanding defect annihilation mechanisms in the formation of these complex structures is also mandatory, as most of the applications require specific and intricate device architectures with a very low level of defectivity. Another challenge is to extend iterative self-assembly to ultra-low dimensions by using "high χ" BCPs

as building blocks while creative macromolecular engineering could enrich the pool of starting morphologies. In summary, this progress report has overviewed exquisite demonstrations of multiple BCP layer self-assembly strategies, however, we also point to the need to define a better understanding of key influencing factors governing precise stack placement. For example, future research and development exploring the surfaces and interfaces of three dimensional BCP features will further allow us to not only advance morphology intricacy, but will also enable us to define limitations of particular systems and approaches. Moreover, given that the "non-native" BCP field is in its infancy, there are many important learnings that will be established in the coming years that will progress the transition to new devices. In particular, we suggest further exploration researching the influence of surface chemistry between stack layers, the effect of using different BCP chemistries and resulting orientation control, and advanced three-dimensional characterization studies (e.g. GISAXS and TEM tomography) will help in the realization of novel device concepts. Such milestones on non-native BCP control coupled with the opportunities inherent to sophisticated functionalization methods will further enhance the viability of multilayered BCP structures for nanotechnologies.

[1]   F. S. Bates, G. H. Fredrickson, *Annu. Rev. Phys. Chem.* **1990**, *41*, 525.

[2]   A. J. Meuler, M. a. Hillmyer, F. S. Bates, *Macromolecules* **2009**, *42*, 7221.

[3]   F. S. Bates, M. a Hillmyer, T. P. Lodge, C. M. Bates, K. T. Delaney, G. H. Fredrickson, *Science* **2012**, *336*, 434.

[4]   L. Leibler, *Macromolecules* **1980**, *13*, 1602.

[5]   M. W. Matsen, M. Schick, *Phys. Rev. Lett.* **1994**, *72*, 2660.

[6]   M. W. Matsen, *Macromolecules* **2012**, *45*, 2161.

[7]   C. Park, J. Yoon, E. L. Thomas, *Polymer* **2003**, *44*, 6725.

[8]   *Block Copolymers in Nanoscience*; Lazzari, M.; Liu, G.; Lecommandoux, S., Eds.; Wiley, 2006.

[9]   I. W. Hamley, Nanotechnology with soft materials. *Angew. Chemie - Int. Ed.* **2003**, *42*, 1692–1712.

[10]   C. Cummins, T. Ghoshal, J. D. Holmes, M. A. Morris, *Adv. Mater.* **2016**, *28*, 5586.

[11]   K. Aissou, T. Alnasser, G. Pecastaings, G. Goglio, O. Toulemonde, S. Mornet, G. Fleury, G. Hadziioannou, *J. Mater. Chem. C* **2013**, *1*, 1317.

[12]   Y. S. Jung, W. Jung, C. A. Ross, *Nano Lett.* **2008**, *8*, 2975.

[13]   J. Y. Cheng, C. A. Ross, V. Z.-H. Chan, E. L. Thomas, R. G. H. Lammertink, G. J. Vancso, *Adv. Mater.* **2001**, *13*, 1174.

[14]   C. T. Black, *Appl. Phys. Lett.* **2005**, *87*, 1.

[15]   J. G. Son, M. Son, K. J. Moon, B. H. Lee, J. M. Myoung, M. S. Strano, M. H. Ham, C. A. Ross, *Adv. Mater.* **2013**, *25*, 4723.

[16]   M. C. Orilall, U. Wiesner, J. Lee, F. J. DiSalvo, U. Wiesner, S. M. Gruner, A. Baiker, U. Wiesner, F. J. DiSalvo, U. Steiner, H. J. Snaith, U. Steiner, H. J. Snaith, *Chem. Soc. Rev.* **2011**, *40*, 520.

[17]   S. Vignolini, N. A. Yufa, P. S. Cunha, S. Guldin, I. Rushkin, M. Stefik, K. Hur, U. Wiesner, J. J. Baumberg, U. Steiner, *Adv. Mater.* **2012**, *24*, OP23.

[18]   J. A. Dolan, B. D. Wilts, S. Vignolini, J. J. Baumberg, U. Steiner, T. D. Wilkinson, *Adv. Opt. Mater.* **2015**, *3*, 12.

[19]   Y. Kang, J. J. Walish, T. Gorishnyy, E. L. Thomas, *Nat. Mater.* **2007**, *6*, 957.

[20]   H. S. Lim, J. H. Lee, J. J. Walish, E. L. Thomas, *ACS Nano* **2012**, *6*, 8933.

[21]   M. Stefik, S. Guldin, S. Vignolini, U. Wiesner, U. Steiner, *Chem. Soc. Rev.* **2015**, *44*, 5076.

[22]   Q. Peng, Y.-C. C. Tseng, S. B. Darling, J. W. Elam, *Adv. Mater.* **2010**, *22*, 5129.

[23]   Q. Peng, Y. C. Tseng, S. B. Darling, J. W. Elam, *ACS Nano* **2011**.

[24]   T. Thurn-Albrecht, J. Schotter, G. A. Kastle, N. Emley, T. Shibauchi, L. Krusin-Elbaum, K. Guarini, C. T. Black, M. T. Tuominen, T. P. Russell, *Science* **2000**, *290*, 2126.

[25]   V. N. Urade, T. C. Wei, M. P. Tate, J. D. Kowalski, H. W. Hillhouse, *Chem. Mater.* **2007**, *19*, 768.

[26]   E. J. W. Crossland, M. Kamperman, M. Nedelcu, C. Ducati, U. Wiesner, D.-M. Smilgies, G. E. S. Toombes, M. A. Hillmyer, S. Ludwigs, U. Steiner, H. J. Snaith, *Nano Lett.* **2009**, *9*, 2807.

[27]   M. Park, P. M. Chaikin, R. A. Register, D. H. Adamson, *Appl. Phys. Lett.* **2001**, *79*, 257.

[28]   K. W. Guarini, C. T. Black, K. R. Milkove, R. L. Sandstrom, *J. Vac. Sci. Technol. B Microelectron. Nanom. Struct.* **2001**, *19*, 2784.

[29]   J. Chai, D. Wang, X. Fan, J. M. Buriak, *Nat. Nanotechnol.* **2007**, *2*, 500.

[30]   J. Chai, J. M. Buriak, *ACS Nano* **2008**, *2*, 489.

[31]   S. B. Darling, N. A. Yufa, A. L. Cisse, S. D. Bader, S. J. Sibener, *Adv. Mater.* **2005**, *17*, 2446.

[32]   N. C. Bigall, B. Nandan, E. B. Gowd, A. Horechyy, A. Eychmüller, *ACS Appl. Mater. Interfaces* **2015**, *7*, 12559.

[33]   H.-Y. Y. Hsueh, H.-Y. Y. Chen, M.-S. S. She, C.-K. K. Chen, R.-M. M. Ho, S. Gwo, H. Hasegawa, E. L. Thomas, *Nano Lett.* **2010**, *10*, 4994.

[34]   A. Haryono, W. H. Binder, *Small* **2006**, *2*, 600.

[35]   Q. Zhang, S. Gupta, T. Emrick, T. P. Russell, *J. Am. Chem. Soc.* **2006**, *128*, 3898.

[36]   K. Thorkelsson, A. J. Mastroianni, P. Ercius, T. Xu, *Nano Lett.* **2012**, *12*, 498.

[37]   K. Aissou, G. Fleury, G. Pecastaings, T. Alnasser, S. Mornet, G. Goglio, G. Hadziioannou, *Langmuir* **2011**, *27*, 14481.

[38]   E. L. Crepaldi, G. J. d. A. A. Soler-Illia, D. Grosso, F. Cagnol, F. Ribot, C. Sanchez, *J. Am. Chem. Soc.* **2003**, *125*, 9770.

[39]   G. J. Galo, E. L. Crepaldi, D. Grosso, C. Sanchez, Block copolymer-templated mesoporous oxides. *Curr. Opin. Colloid Interface Sci.* **2003**, *8*, 109–126.

[40]   J. Lee, M. Christopher Orilall, S. C. Warren, M. Kamperman, F. J. Disalvo, U. Wiesner, *Nat. Mater.* **2008**, *7*, 222.

[41]   C. Sinturel, M. Vayer, M. Morris, M. A. Hillmyer, *Macromolecules* **2013**, *46*, 5399.

[42]   C. Tang, W. Wu, D.-M. M. Smilgies, K. Matyjaszewski, T. Kowalewski, *J. Am. Chem. Soc.* **2011**, *133*, 11802.

[43]   P. W. Majewski, K. G. Yager, *ACS Nano* **2015**, *9*, 3896.

[44]   D. E. Angelescu, J. H. Waller, D. H. Adamson, P. Deshpande, S. Y. Chou, R. A. Register, P. M. Chaikin, *Adv. Mater.* **2004**, *16*, 1736.

[45] D. E. Angelescu, J. H. Waller, R. A. Register, P. M. Chaikin, *Adv. Mater.* **2005**, *17*, 1878.

[46] T. L. Morkved, M. Lu, A. M. Urbas, E. E. Ehrichs, H. M. Jaeger, P. Mansky, T. P. Russell, *Science* **1996**, *273*, 931.

[47] H. U. Jeon, H. M. Jin, J. Y. Kim, S. K. Cha, J. H. Mun, K. E. Lee, J. J. Oh, T. Yun, J. S. Kim, S. O. Kim, *Mol. Syst. Des. Eng.* **2017**, *2*, 560.

[48] P. W. Majewski, M. Gopinadhan, C. O. Osuji, *J. Polym. Sci. Part B Polym. Phys.* **2012**, *50*, 2.

[49] M. Gopinadhan, Y. Choo, L. H. Mahajan, D. Ndaya, G. Kaufman, Y. Rokhlenko, R. M. Kasi, C. O. Osuji, *Mol. Syst. Des. Eng.* **2017**, *2*, 549.

[50] P. Mansky, Y. Lui, E. Huang, T. P. Russell, C. J. Hawker, *Science* **1997**, *275*, 1458.

[51] C. M. Bates, T. Seshimo, M. J. Maher, W. J. Durand, J. D. Cushen, L. M. Dean, G. Blachut, C. J. Ellison, C. G. Willson, *Science* **2012**, *338*, 775.

[52] S. Park, D. H. Lee, J. Xu, B. Kim, S. W. Hong, U. Jeong, T. Xu, T. P. Russell, *Science* **2009**, *323*, 1030.

[53] K. Aissou, J. Shaver, G. Fleury, G. Pécastaings, C. Brochon, C. Navarro, S. Grauby, J.-M. Rampnoux, S. Dilhaire, G. Hadziioannou, *Adv. Mater.* **2013**, *25*, 213.

[54] S. O. Kim, H. H. Solak, M. P. Stoykovich, N. J. Ferrier, J. J. De Pablo, P. F. Nealey, *Nature* **2003**, *424*, 411.

[55] C.-C. Liu, E. Han, M. S. Onses, C. J. Thode, S. Ji, P. Gopalan, P. F. Nealey, *Macromolecules* **2011**, *44*, 1876.

[56] R. A. Segalman, H. Yokoyama, E. J. Kramer, *Adv. Mater.* **2001**, *13*, 1152.

[57] J. Y. Cheng, C. a. Ross, E. L. Thomas, H. I. Smith, G. J. Vancso, *Appl. Phys. Lett.* **2002**, *81*, 3657.

[58] S. B. Darling, *Prog. Polym. Sci.* **2007**, *32*, 1152.

[59] *Directed Self-assembly of Block Co-polymers for Nano-manufacturing*; Gronheid, R.; Nealey, P., Eds.; Elsevier, 2015.

[60] H. Hu, M. Gopinadhan, C. O. Osuji, *Soft Matter* **2014**, *10*, 3867.

[61] W. Li, M. Müller, *Prog. Polym. Sci.* **2016**, *54–55*, 47.

[62] *Functional Organic and Hybrid Nanostructured Materials*; Li, Q., Ed.; Wiley-VCH Verlag GmbH & Co. KGaA: Weinheim, Germany, 2018.

[63] A. Karim, N. Singh, M. Sikka, F. S. Bates, W. D. Dozier, G. P. Felcher, *J. Chem. Phys.* **1994**, *100*, 1620.

[64] L. H. Radzilowski, B. L. Carvalho, E. L. Thomas, *J. Polym. Sci. Part B Polym. Phys.* **1996**, *34*, 3081.

[65] M. W. Matsen, *Curr. Opin. Colloid Interface Sci.* **1998**, *3*, 40.

[66] A. Knoll, A. Horvat, K. S. Lyakhova, G. Krausch, G. J. A. Sevink, A. V Zvelindovsky, R. Magerle, *Phys. Rev. Lett.* **2002**, *89*, 035501.

[67] G. E. Stein, E. J. Kramer, X. Li, J. Wang, *Macromolecules* **2007**, *40*, 2453.

[68] W. Bai, C. A. Ross, *MRS Bull.* **2016**, *41*, 100.

[69] G. S. Doerk, K. G. Yager, *Mol. Syst. Des. Eng.* **2017**, *2*, 518.

[70] J. H. Kim, H. M. Jin, G. G. Yang, K. H. Han, T. Yun, J. Y. Shin, S. Jeong, S. O. Kim, *Adv. Funct. Mater.* **2019**, 1902049.

[71] K. Hayashida, A. Takano, S. Arai, Y. Shinohara, Y. Amemiya, Y. Matsushita, *Macromolecules* **2006**, *39*, 9402.

[72] Y. Matsushita, *Macromolecules* **2007**, *40*, 771.

[73] B. R. Sveinbjörnsson, R. a Weitekamp, G. M. Miyake, Y. Xia, H. a Atwater, R. H. Grubbs, *Proc. Natl. Acad. Sci. U. S. A.* **2012**, *109*, 14332.

[74] W. Gu, J. Huh, S. W. Hong, B. R. Sveinbjornsson, C. Park, R. H. Grubbs, T. P. Russell, *ACS Nano* **2013**, *7*, 2551.

[75] K. Aissou, W. Kwon, M. Mumtaz, S. Antoine, M. Maret, G. Portale, G. Fleury, G. Hadziioannou, *ACS Nano* **2016**, *10*, 4055.

[76] S. Antoine, K. Aissou, M. Mumtaz, G. Pécastaings, T. Buffeteau, G. Fleury, G. Hadziioannou, *Macromol. Rapid Commun.* **2019**, *40*, 1800860.

[77] S. Salahuddin, K. Ni, S. Datta, *Nat. Electron.* **2018**, *1*, 442.

[78] R. Clark, K. Tapily, K. H. Yu, T. Hakamata, S. Consiglio, D. O'Meara, C. Wajda, J. Smith, G. Leusink, *APL Mater.* **2018**, *6*.

[79] T. N. Theis, H. S. Philip Wong, *Comput. Sci. Eng.* **2017**, *19*, 41.

[80] C. Cummins, M. A. Morris, Using block copolymers as infiltration sites for development of future nanoelectronic devices: Achievements, barriers, and opportunities. *Microelectron. Eng.* **2018**, *195*, 74–85.

[81] H.-Y. Y. Hsueh, C.-T. T. Yao, R.-M. M. Ho, *Chem. Soc. Rev.* **2015**, *44*, 1974.

[82] T. Ito, G. Ghimire, Electrochemical Applications of Microphase-Separated Block Copolymer Thin Films. *ChemElectroChem* **2018**, *5*, 2937–2953.

[83] H. Hu, S. Rangou, M. Kim, P. Gopalan, V. Filiz, A. Avgeropoulos, C. O. Osuji, *ACS Nano* **2013**, *7*, 2960.

[84] Y. Choo, H. Hu, K. Toth, C. O. Osuji, *J. Polym. Sci. Part B Polym. Phys.* **2016**, *54*, 247.

[85] A. Tavakkoli K. G., K. W. Gotrik, A. F. Hannon, A. Alexander-Katz, C. A. Ross, K. K. Berggren, *Science* **2012**, *336*, 1294.

[86] J. W. Jeong, W. I. Park, L.-M. M. Do, J.-H. H. Park, T.-H. H. Kim, G. Chae, Y. S. Jung, *Adv. Mater.* **2012**, *24*, 3526.

[87] J. Y. Kim, B. H. Kim, J. O. Hwang, S. J. Jeong, D. O. Shin, J. H. Mun, Y. J. Choi, H. M. Jin, S. O. Kim, *Adv. Mater.* **2013**, *25*, 1331.

[88] P. W. Majewski, A. Rahman, C. T. Black, K. G. Yager, *Nat. Commun.* **2015**, *6*, 7448.

[89] A. Tavakkoli K. G., S. M. Nicaise, A. F. Hannon, K. W. Gotrik, A. Alexander-Katz, C. A. Ross, K. K. Berggren, *Small* **2014**, *10*, 493.

[90] A. A. Abate, G. T. Vu, A. D. Pezzutti, N. A. García, R. L. Davis, F. Schmid, R. A. Register, D. A. Vega, *Macromolecules* **2016**, *49*, 7588.

[91] F. Rose, J. K. Bosworth, E. A. Dobisz, R. Ruiz, *Nanotechnology* **2011**, *22*, 035603.

[92] E. Kim, C. Shin, H. Ahn, D. Y. Ryu, J. Bang, C. J. Hawker, T. P. Russell, *Soft Matter* **2008**, *4*, 475.

[93] H. Jung, D. Hwang, E. Kim, B.-J. Kim, W. B. Lee, J. E. Poelma, J. Kim, C. J. Hawker, J. Huh, D. Y. Ryu, J. Bang, *ACS Nano* **2011**, *5*, 6164.

[94] C. He, M. P. Stoykovich, *Adv. Funct. Mater.* **2014**, *24*, 7078.

[95] Y. J. Choi, J. Y. Kim, J. E. Kim, J. H. Mun, S. K. Cha, S. O. Kim, *Adv. Funct. Mater.* **2016**, *26*, 6462.

[96] H. Jung, S. Woo, S. Park, S. Lee, M. Kang, Y. Choe, J. G. Son, D. Y. Ryu, J. Huh, J. Bang, *Soft Matter* **2015**, *11*, 4242.

[97] S. Y. Kim, A. Nunns, J. Gwyther, R. L. Davis, I. Manners, P. M. Chaikin, R. A. Register, *Nano Lett.* **2014**, *14*, 5698.

[98] J. Oh, H. S. Suh, Y. Ko, Y. Nah, J. C. Lee, B. Yeom, K. Char, C. A. Ross, J. G. Son, *Nat. Commun.* **2019**, *10*, 2912.

[99] A. Rahman, P. W. Majewski, G. Doerk, C. T. Black, K. G. Yager, *Nat. Commun.* **2016**, *7*, 13988.

[100] R. Ruiz, R. L. Sandstrom, C. T. Black, *Adv. Mater.* **2007**, *19*, 587.

[101] S. M. Park, P. Ravindran, Y. H. La, G. S. W. Craig, N. J. Ferrier, P. F. Nealey, *Langmuir* **2007**, *23*, 9037.

[102] Y. S. Jung, J. B. Chang, E. Verploegen, K. K. Berggren, C. A. Ross, *Nano Lett.* **2010**, *10*, 1000.

[103] J. G. Son, A. F. Hannon, K. W. Gotrik, A. Alexander-Katz, C. A Ross, *Adv. Mater.* **2011**, *23*, 634.

[104] A. Tavakkoli K. G., S. M. Nicaise, K. R. Gadelrab, A. Alexander-Katz, C. A. Ross, K. K. Berggren, *Nat. Commun.* **2016**, *7*, 10518.

[105] D. O. Shin, J. H. Mun, G.-T. Hwang, J. M. Yoon, J. Y. Kim, J. M. Yun, Y. Yang, Y. Oh, J. Y. Lee, J. Shin, K. J. Lee, S. Park, J. U. Kim, S. O. Kim, *ACS Nano* **2013**, *7*, 8899.

[106] C. Jin, B. C. Olsen, N. L. Y. Wu, E. J. Luber, J. M. Buriak, *Langmuir* **2016**, *32*, 5890.

[107] H. Jung, W. H. Shin, T. W. Park, Y. J. Choi, Y. J. Yoon, S. H. Park, J. H. Lim, J. D.

Kwon, J. W. Lee, S. H. Kwon, G. H. Seong, K. H. Kim, W. I. Park, *Nanoscale* **2019**, *11*, 8433.

[108] C. Jin, B. C. Olsen, E. J. Luber, J. M. Buriak, *ACS Nano* **2017**, *11*, 3237.

[109] J. Y. Kim, H. Kim, B. H. Kim, T. Chang, J. Lim, H. M. Jin, J. H. Mun, Y. J. Choi, K. Chung, J. Shin, S. Fan, S. O. Kim, *Nat. Commun.* **2016**, *7*, 12911.

[110] A. Alvarez-Fernandez, K. Aissou, G. Pécastaings, G. Hadziioannou, G. Fleury, V. Ponsinet, *Nanoscale Adv.* **2019**, *1*, 849.

[111] S. J. Jeong, S. Jo, J. Lee, K. Yang, H. Lee, C. S. Lee, H. Park, S. Park, *Nano Lett.* **2016**, *16*, 5378.

[112] J. Arias-Zapata, J. D. Garnier, H. Al Mehedi, A. Legrain, B. Salem, G. Cunge, M. Zelsmann, *Chem. Mater.* **2019**, *31*, 3154.

[113] K. V. Peinemann, V. Abetz, P. F. W. Simon, *Nat. Mater.* **2007**, *6*, 992.

[114] C. Zhou, T. Segal-Peretz, M. E. Oruc, H. S. Suh, G. Wu, P. F. Nealey, *Adv. Funct. Mater.* **2017**, *27*, 1701756.

[115] K. Aissou, M. Mumtaz, H. Bouzit, G. Pécastaings, G. Portale, G. Fleury, G. Hadziioannou, *Macromolecules* **2019**, *52*, 4413.

[116] S. B. Darling, *Energy Environ. Sci.* **2009**, *2*, 1266.

[117] S. W. Robbins, P. A. Beaucage, H. Sai, K. W. Tan, J. G. Werner, J. P. Sethna, F. J. DiSalvo, S. M. Gruner, R. B. Van Dover, U. Wiesner, *Sci. Adv.* **2016**, *2*, e1501119.